Supporting Online Material

All-optical electrophysiology in mammalian neurons using engineered microbial rhodopsins

Daniel R. Hochbaum[*], Yongxin Zhao[*], Samouil L. Farhi, Nathan Klapoetke, Christopher A. Werley, Vikrant Kapoor, Peng Zou, Joel M. Kralj, Dougal Maclaurin, Niklas Smedemark-Margulies, Jessica L. Saulnier, Gabriella L. Boulting, Christoph Straub, Yongku Cho, Michael Melkonian, Gane Ka-Shu Wong, D. Jed Harrison, Venkatesh N. Murthy, Bernardo Sabatini, Edward S. Boyden[‡], Robert E. Campbell[‡†], Adam E. Cohen[§]

[*]These authors contributed equally to this work. [‡]These authors jointly directed this work.
† For correspondence regarding directed evolution of Arch: robert.e.campbell@ualberta.ca
[§]cohen@chemistry.harvard.edu

Contents

Supplementary Figure 1

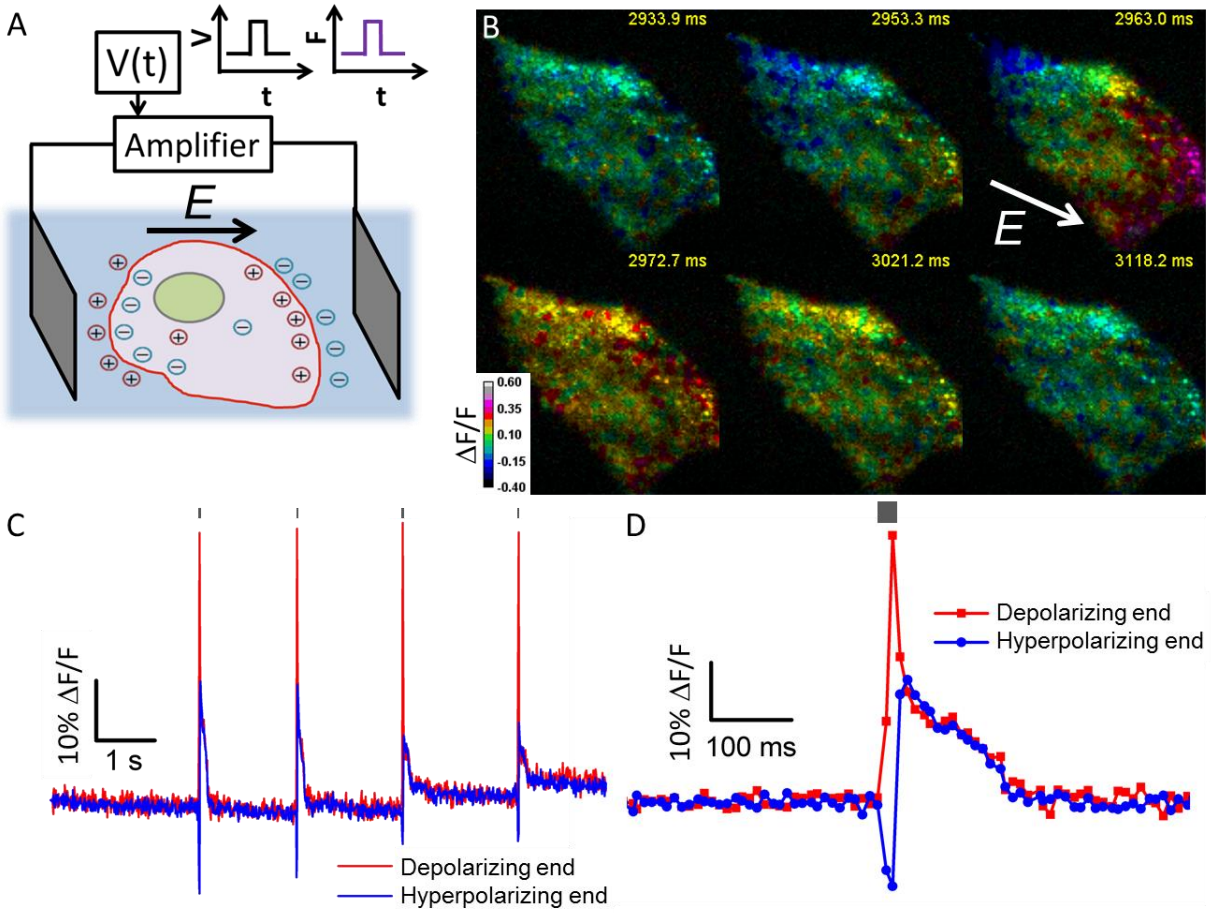

Induced transmembrane voltage (ITV) in Arch-expressing HeLa cells. A) Experimental setup, showing two platinum electrodes placed on either side of a transfected cell. *V(t)* represents the pulse generator and high-voltage amplifier. B) Frames from a movie of a HeLa cell expressing QuasAr1. The cell was stimulated with an electrical pulse (20 ms, 50 V/cm). The images show the fluorescence response (Δ*F/F*). The arrow labeled 'E' indicates the direction of the electric field. C) Fluorescence of the cell poles during the ITV experiment shown in (B). Gray marks above the fluorescence traces indicate timing and duration of the ITV pulses. D) Expanded view of one fluorescence intensity peak from (C).

Supplementary Figure 2

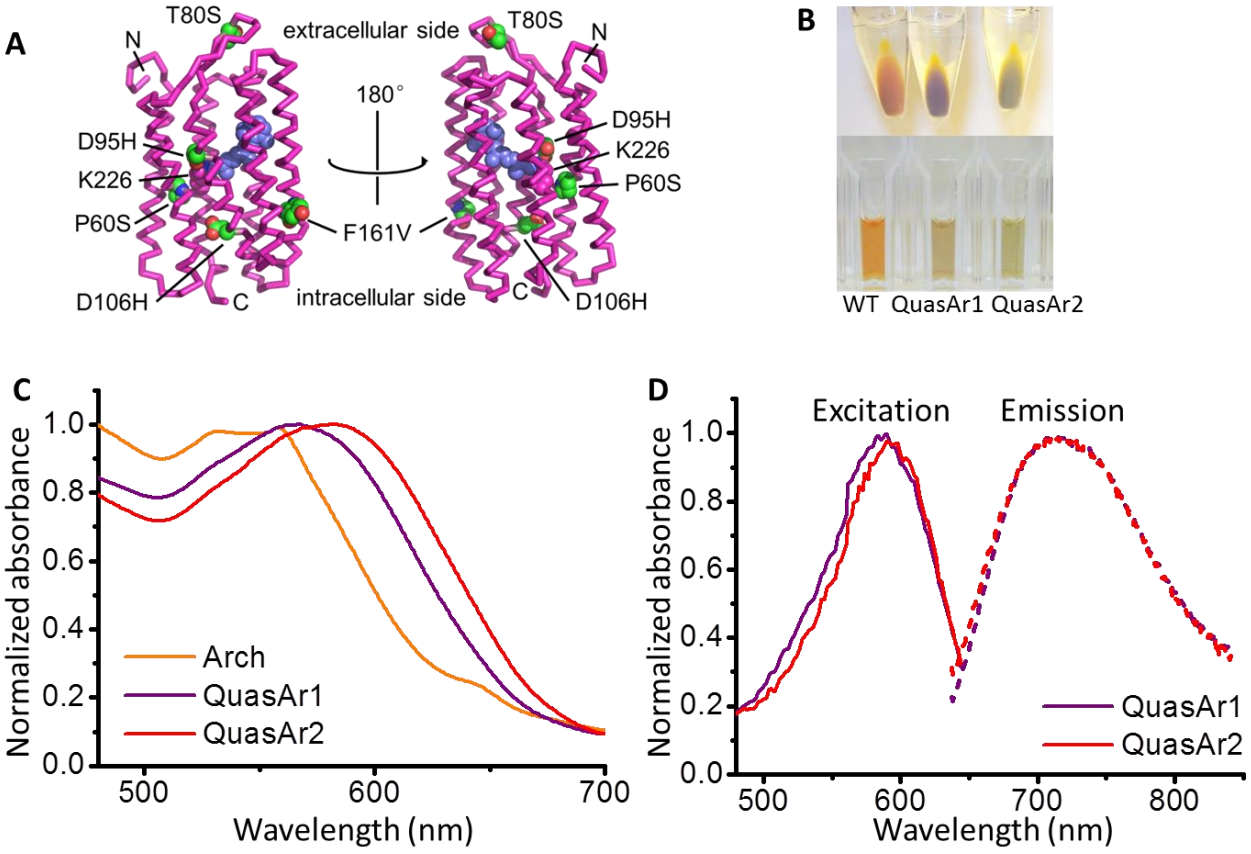

Structural and spectroscopic properties of QuasArs. A) Locations of mutations in QuasAr1, modeled on the crystal structure of Arch-2 (PDB: 2EI4) [1]. Arch-2 has 90% amino acid identity with Arch-3. The retinal chromophore is colored blue and mutations are colored green. B) Top: Images of *E. coli* pellets expressing Arch, QuasAr1, and QuasAr2. Bottom: Images of solubilized protein. C) Absorption spectra of Arch, QuasAr1 and QuasAr2, measured on solubilized protein. D) Excitation and emission spectra measured on QuasAr1 and QuasAr2. Arch was too dim to measure in the fluorimeter. Emission spectra were recorded with λ_{exc} = 600 nm. Excitation spectra were measured with λ_{em} = 750 nm.

Supplementary Figure 3

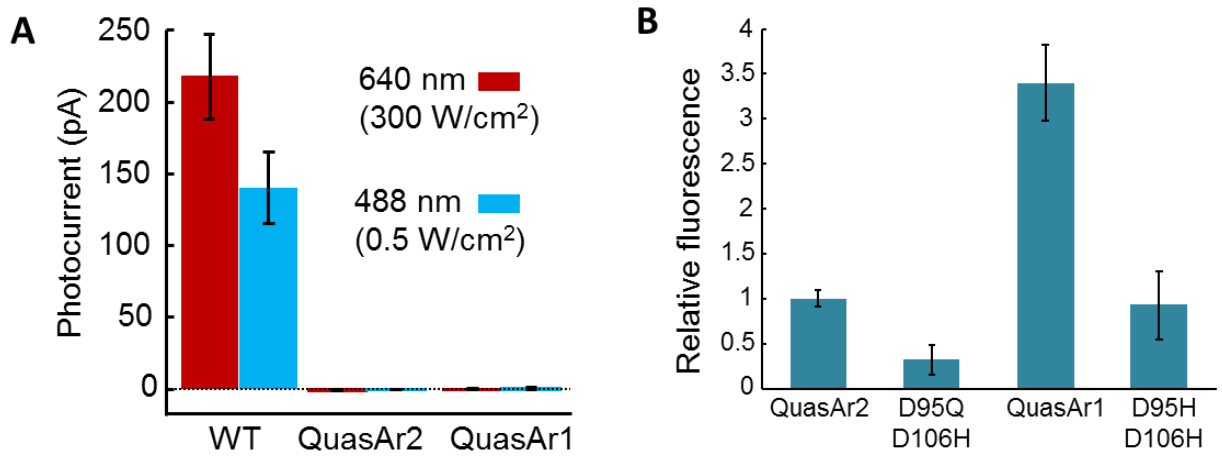

Photophysics of QuasArs in mammalian cells. A) In cultured rat hippocampal neurons, wild-type Arch generated photocurrents of 220 ± 30 pA (*n* = 6 cells) under red illumination (1 s, 640 nm, 300 W/cm^2) and 140 ± 25 pA under blue light (1 s, 488 nm, 500 mW/cm^2). Steady state photocurrents were calculated by averaging the current over the last 0.25 seconds of light exposure and subtracting the holding current (cells held at -65 mV) in the dark. These currents hyperpolarized cells by 25 ± 4 mV and 19 ± 3 mV, respectively. Neither QuasAr1 (*n* = 9 cells) nor QuasAr2 (*n* = 7 cells) generated detectable photocurrents under either illumination condition, nor under red illumination at up to 900 W/cm^2. B) Comparison of fluorescence between QuasAr mutants and Arch double mutants, expressed as eGFP fusions in HEK cells. The double mutants had mutations at the locations of the proton acceptor (Asp95) and proton donor (Asp106) to the Schiff base. QuasAr1 includes mutations D95H, D106H, and QuasAr2 includes mutations D95Q, D106H. The three additional backbone mutations in the QuasArs (P60S, T80S, F161V) increased brightness relative to the double mutants. Fluorescence of each Arch mutant was measured with excitation at 640 nm and emission from 660 – 760 nm. To control for variation in expression level, fluorescence was normalized by eGFP fluorescence (λ_{exc} = 488 nm, λ_{em} = 510 – 550 nm). Error bars represent s.e.m. for measurements on *n* = 5 - 10 cells.

Supplementary Figure 4

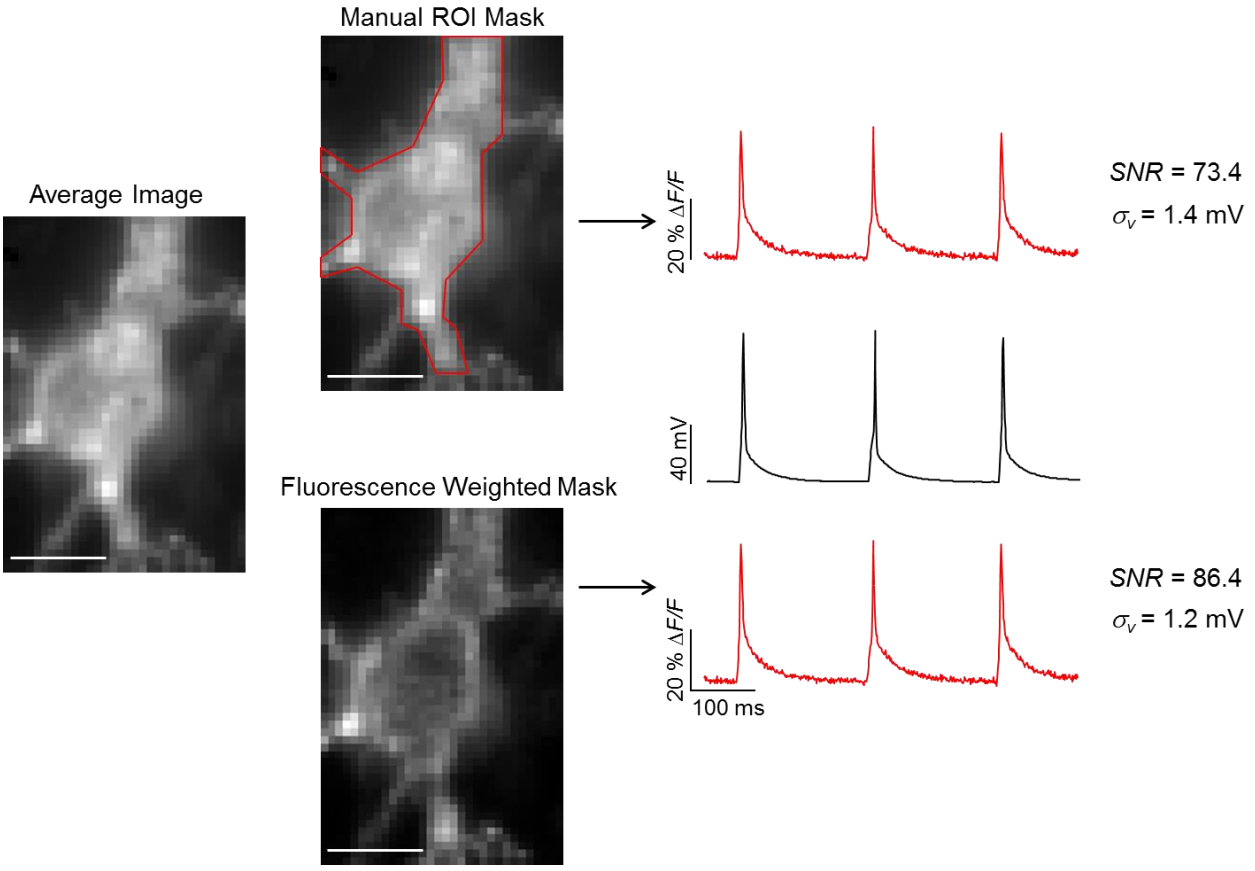

Extraction of fluorescence traces from QuasAr movies. Fluorescence can either be calculated by manually defining a region of interest (ROI; top row), or by preferentially weighting the pixels whose intensity co-varies with the whole-field average (bottom row)[2]. The noise in the fluorescence trace when scaled to match the electrical recording is denoted σ_v. With the improved trafficking of the QuasAr mutants compared to Arch, the automated technique gave only slightly higher SNR than manual definition of the ROI. The technique makes no use of the electrode readout. Cell shown is the source of the data in **Fig. 1g**. All comparisons of SNR in culture were made on measurements taken at the same magnification (60x), collected on the same EMCCD (**Methods**), and extracted using this automated technique. For recordings on cultured neurons, values of $\Delta F/F$ were calculated after subtracting background autofluorescence from a cell-free region of the field of view. This background subtraction was not performed on recordings in tissue.

Supplementary Figure 5

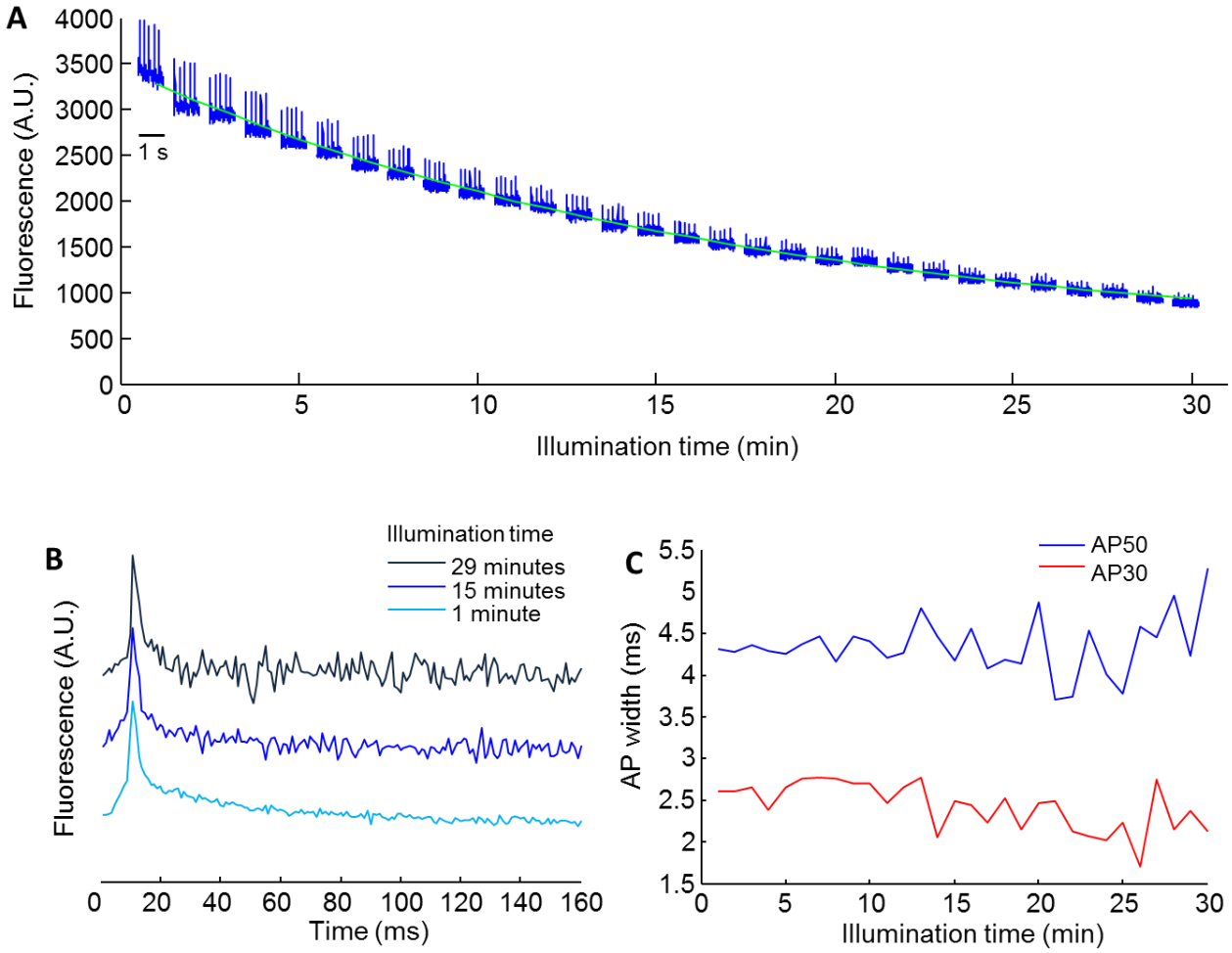

Photobleaching of QuasAr2 and test for red light induced phototoxicity. A) Fluorescence traces from a neuron expressing QuasAr2 and CheRiff (Optopatch2, described below), with APs induced via blue light activation of the CheRiff. Optogenetic stimulation was preferable to manual patch clamp due to the poor stability of patch connections over long-term measurements. The cell was illuminated for 30 minutes continuously at 640 nm, 300 W/cm^2 and probed at 60 s intervals with blue light to induce a burst of APs (5 pulses of 10 ms, 5 Hz, 20 mW/cm^2). The cell fired APs with 100% fidelity over the recording period, though the signal-to-noise ratio decreased as the QuasAr2 fluorescence dropped. B) Fluorescence traces of APs at the beginning, middle, and end of the recording in (A). Each trace in (B) is an average of the 5 APs elicited during that time point. C) AP widths measured at 30% and 50% recovery from peak fluorescence deviation. APs did not show a detectable change in width over the 30-minute recording.

Supplementary Figure 6

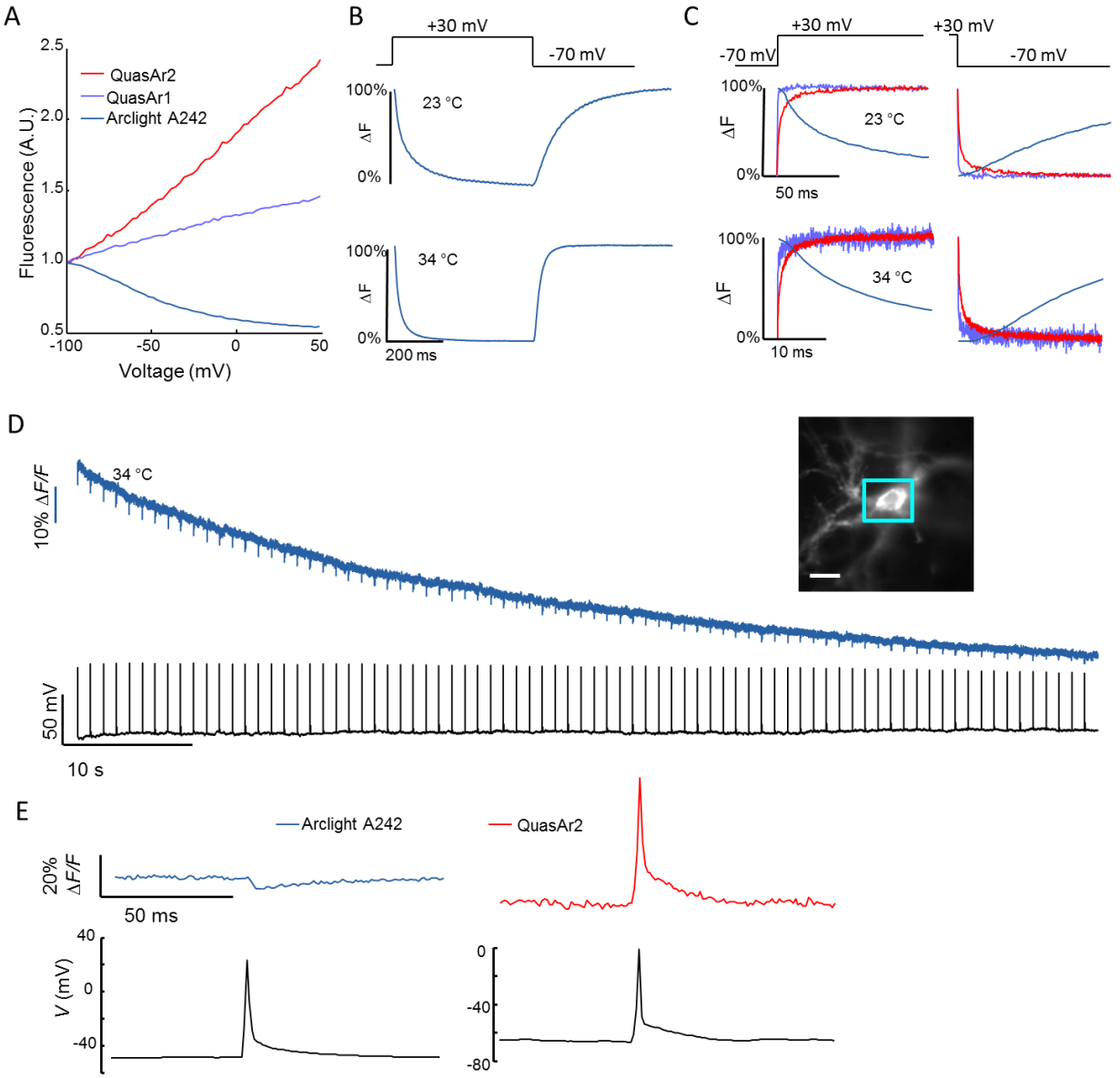

Comparison of voltage-indicating properties of QuasArs and ArcLight A242 in culture. A) Fluorescence as a function of membrane voltage in HEK293T cells. ArcLight showed voltage sensitivity of -32 ± 3% ΔF/F per 100 mV (n = 7 cells), comparable in magnitude to QuasAr1 and 2.8-fold smaller than QuasAr2. B) Response of ArcLight to steps in membrane voltage. ArcLight showed bi-exponential kinetics in response to rising or falling voltage steps (**Supplementary Table 2**). Mean half-response times were 42 ± 8 ms and 76 ± 5 ms on rising and falling edges at 23 °C (n = 6 cells) and 11 ± 1 and 17 ± 2 ms on rising and falling edges at 34 °C (n = 7 cells). C) Step responses of ArcLight and QuasArs overlaid on the same time axis at 23 °C (top) and 34 °C (bottom). D) Continuous illumination of a neuron expressing ArcLight (488 nm, 10 W/cm^2) led to photobleaching with a time constant of 70 s. Inset: Low-

magnification image of the neuron. Scale bar 20 μm. Cyan box shows field of view used for high-speed (1 kHz frame rate) movies of fluorescence dynamics. Fluorescence was calculated using the same pixel weighting algorithm used for QuasAr data (**Supplementary Fig. 4**). E) Single-trial fluorescence response of ArcLight (blue) and QuasAr2 (red) to a single AP (black), recorded at 34 °C and a 1 kHz frame rate. ArcLight reported action potentials with an amplitude of $\Delta F/F$ = -2.7 ± 0.5% (n = 5 cells) and a single-trial signal-to-noise ratio (SNR) of 8.8 ± 1.6 (488 nm, 10 W/cm^2). ArcLight distorted the AP waveforms to have a width of 14.5 ± 3.0 ms at 70% maximal fluorescence deviation, compared to the true width of 1.3 ± 0.1 ms simultaneously recorded with a patch pipette. QuasAr2 reported APs at 34 °C and 23 °C with comparable single-trial SNR (SNR at 34 °C: 41 ± 3, 300 W/cm^2, n = 8 cells).

Supplementary Figure 7

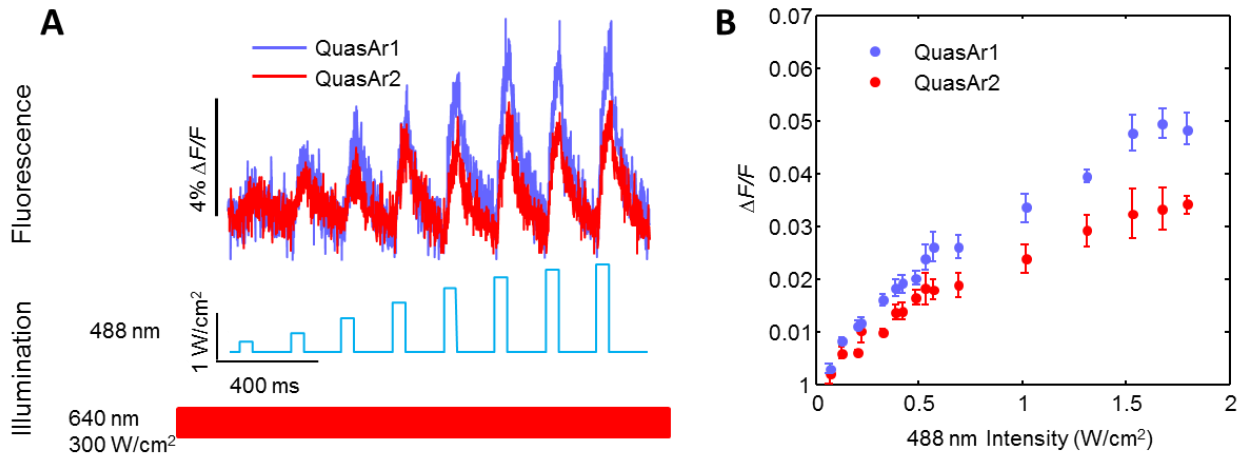

Quantification of optical crosstalk of blue illumination into QuasAr fluorescence. A) Effect of blue illumination on QuasAr fluorescence. HEK293T cells expressing QuasAr1 or QuasAr2 were exposed to continuous excitation at 640 nm (300 W/cm^2) and pulses of illumination at 488 nm (50 ms, 5 Hz). The intensity of the blue pulses increased from 0.06 to 1.8 W/cm^2. B) Quantification of crosstalk. Illumination with blue light at maximum intensity used to excite CheRiff (0.2 W/cm^2) increased QuasAr1 fluorescence by 1.1% and QuasAr2 fluorescence by 0.6%. Initiation of precisely timed APs with existing channelrhodopsins required whole-cell illumination at 0.5 to 2 W/cm^2 (ref. 3). Blue illumination at 1 W/cm^2 increased QuasAr1 fluorescence by 3.4% and QuasAr2 fluorescence by 2.4%, unacceptably high levels of optical crosstalk. Error bars represent s.e.m. for n = 5 cells for each QuasAr. Quantification is given in **Supplementary Table 5**.

Supplementary Figure 8

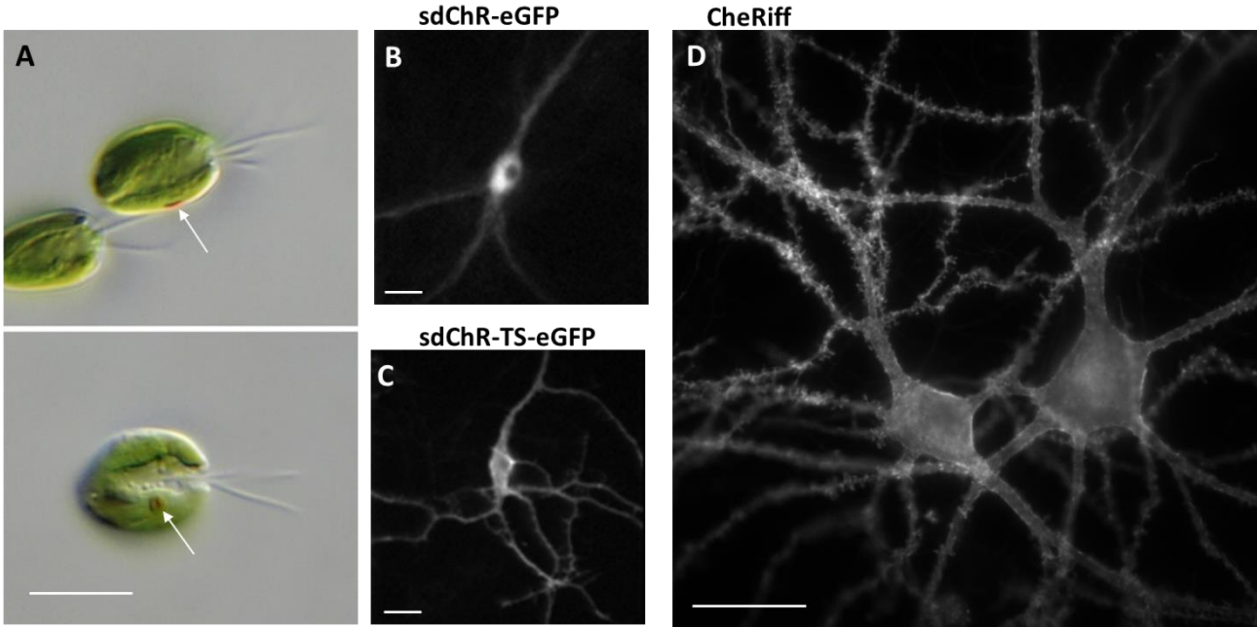

Improvements in trafficking leading to CheRiff. A) Light micrographs (DIC) of *Scherffelia dubia* (strain CCAC 0053) in side view (top) and face view (bottom). Arrows mark eyespots (red). Scale bar 10 μm. Strain and micrographs courtesy of CCAC [http://www.ccac.uni-koeln.de/] and Sebastian Hess (Cologne Biocenter), respectively. B) Image of a cultured neuron expressing wild-type *Scherffelia dubia* Channelrhodopsin (sdChR). SdChR typically aggregated and formed puncta in the soma. Scale bar 25 μm. C) Image of a neuron expressing sdChR with an additional trafficking sequence from Kir2.1 between the C-terminus of sdChR and the N-terminus of eGFP (**Methods**). This trafficking sequence substantially reduced intracellular puncta. Scale bar 25 μm. D) Two neurons expressing CheRiff. Inclusion of the E154A mutation reduced red light sensitivity and reduced τ_{off} while maintaining excellent membrane trafficking and blue light sensitivity. Scale bar 25 μm.

Supplementary Figure 9

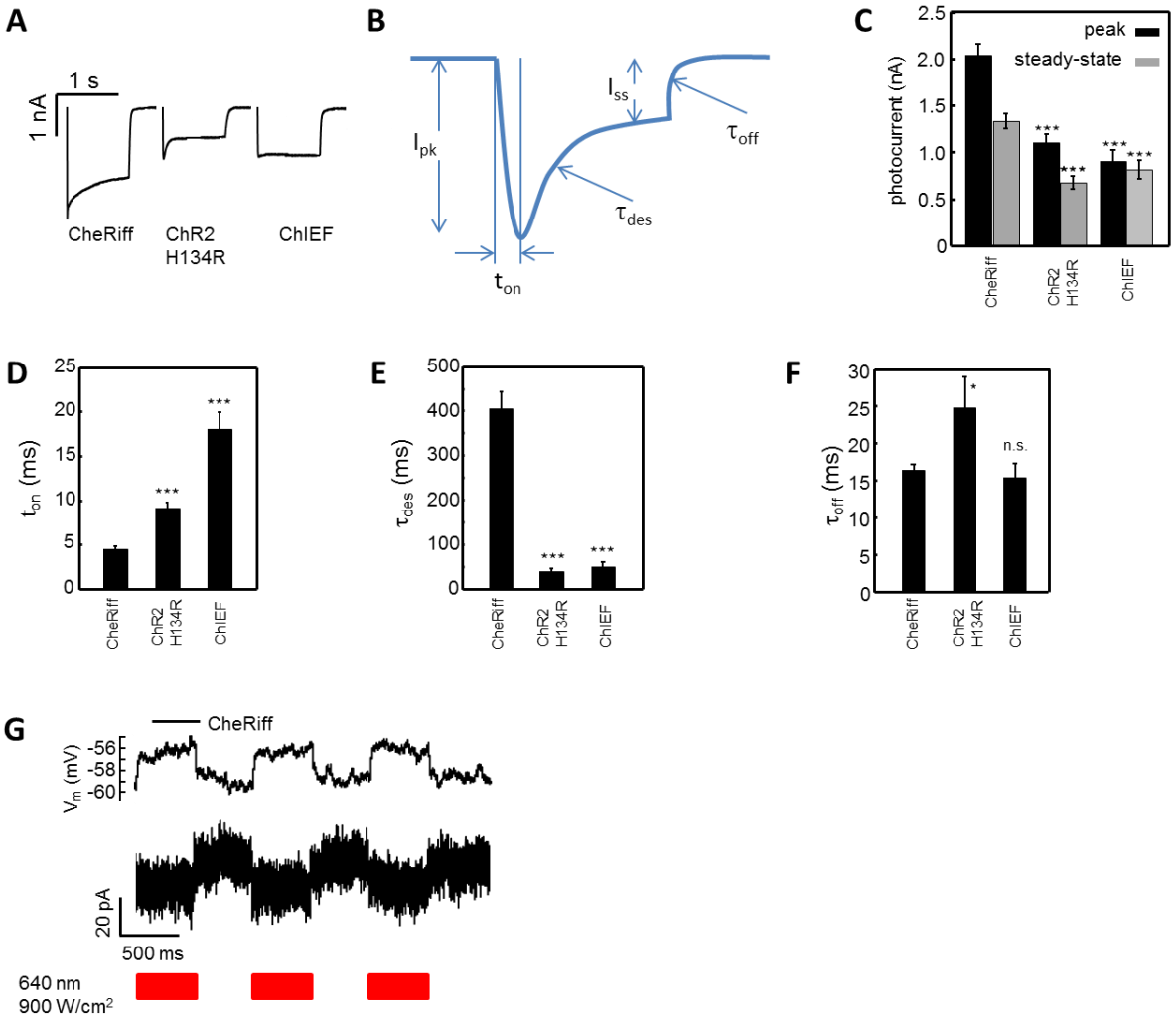

Spectroscopic and kinetic properties of CheRiff. A) Photocurrents measured in response to a 1 second 488 nm light pulse with intensity 500 mW/cm^2, sufficient to open all the channels. Comparisons were made on matched rat hippocampal cultures, DIV 14-15. Expression was driven by a *CaMKIIα* promoter in identical plasmid backbones. See **Methods** for details on cell culture. B) Components of channelrhodopsin current elicited by a step in blue light. I_{pk} is the difference between baseline current and peak current. t_{on} is the time between light onset and peak current. τ_{des} is the desensitization time constant determined by a single-exponential fit to the current decay after the peak. I_{ss} is steady state photocurrent. τ_{off} is the channel closing time constant determined by a single-exponential fit to the current decay after the illumination ceases.

C) Peak (I_{pk}) and steady state (I_{ss}) photocurrents in neurons expressing CheRiff (*n* = 10 cells), ChR2 H134R (*n* = 8 cells), and ChIEF (*n* = 6 cells). CheRiff generated peak photocurrent of 2.0 ± 0.1 nA, approximately 2-fold larger than the peak photocurrents of ChR2 H134R (1.1 ± 0.1

nA, $P < 0.001$) or ChIEF[4] (0.9 ± 0.1 nA, $P < 0.001$). CheRiff also generated significantly larger steady state photocurrents (1.3 ± 0.08 nA) than ChR2 H134R (0.68 ± 0.07 nA, $P < 0.001$) or ChIEF (0.81 ± 0.10 nA, $P < 0.001$).

We further compared the kinetics of CheRiff to ChR2 H134R and to ChIEF under standard channelrhodopsin illumination conditions (488 nm, 500 mW/cm^2) at 23 °C in cultured neurons. D) In response to a step in illumination, CheRiff reached peak photocurrent in 4.5 ± 0.3 ms (n = 10 cells), significantly faster than ChR2 H134R (8.9 ± 0.5 ms, n = 8 cells, $P < 0.001$) or ChiEF (18 ± 1.5 ms, n = 6 cells, $P < 0.001$). E) Under continuous illumination CheRiff partially desensitized with a time constant of 400 ms. ChR2 H134R and ChIEF desensitized significantly faster (39 ± 4 ms, n = 8 cells, $P < 0.001$, and 49 ± 8 ms, n = 5 cells, $P < 0.001$, respectively). F) τ_{off} was measured in response to a 5 ms illumination pulse (500 mW/cm^2) as in ref. 3. Channel closing time constant was comparable between CheRiff and ChIEF (16 ± 0.8 ms, n = 9 cells, and 15 ± 2 ms, n = 6 cells, respectively, $P = 0.94$), and faster than ChR2 H134R (25 ± 4 ms, n = 6 cells, $P < 0.05$). Error bars represent s.e.m. Statistical significance determined by one way ANOVA with Dunnett's post hoc test using CheRiff as the reference. * $P < 0.05$; ** $P < 0.01$; *** $P < 0.001$. **Supplementary Table 4** contains a summary of the comparisons between CheRiff, ChR2 H134R, and ChIEF.

G) Activation of CheRiff by red light used for imaging QuasArs (640 nm, 900 W/cm^2). Top: Under current-clamp (i = 0) in a neuron expressing CheRiff, pulses of red light led to a small steady depolarization of 3.1 ± 0.2 mV (n = 5 cells). Bottom. Under voltage-clamp (V = -65 mV), pulses of red light led to a small inward photocurrent of 14.3 ± 3.1 pA (n = 5 cells).

Supplementary Figure 10

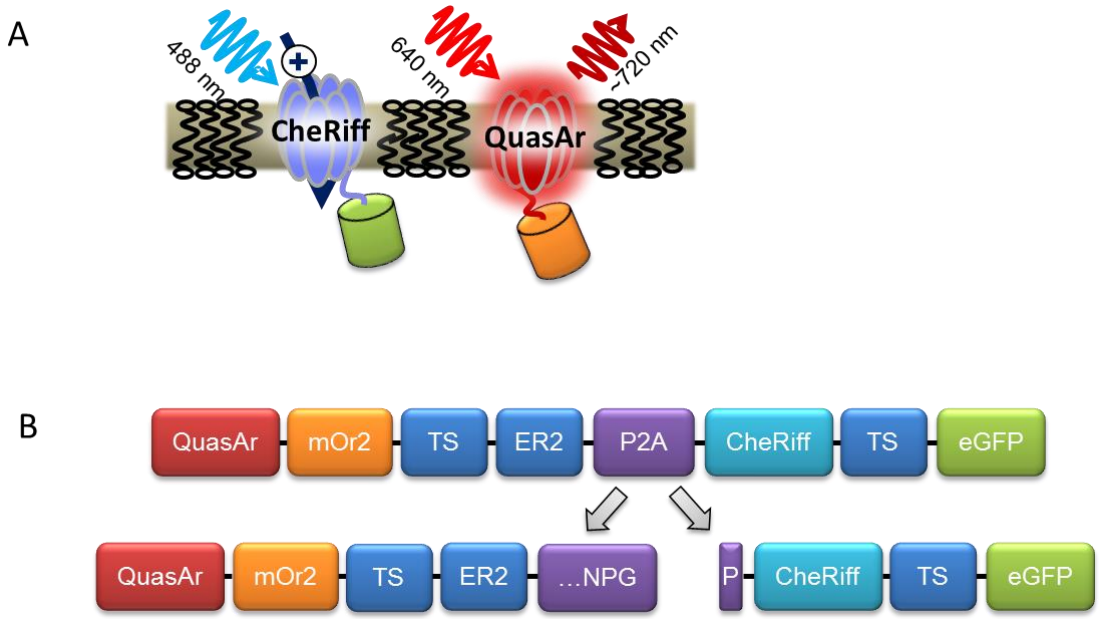

Optopatch construct. A) The optopatch constructs led to co-expression of CheRiff and QuasAr in the cell plasma membrane. CheRiff mediates blue light-induced depolarization. QuasAr reports voltage fluctuations under 640 nm excitation with emission between 660 nm and 760 nm. B) The bicistronic vector consists of a QuasAr fused to mOrange2 with the TS and ER2 trafficking motifs followed by a porcine teschovirus-1 (P2A) sequence, and ending with CheRiff fused to eGFP. The P2A peptide causes a ribosomal skip, leading to approximately stoichiometric co-expression of the actuator and reporter.

Supplementary Figure 11

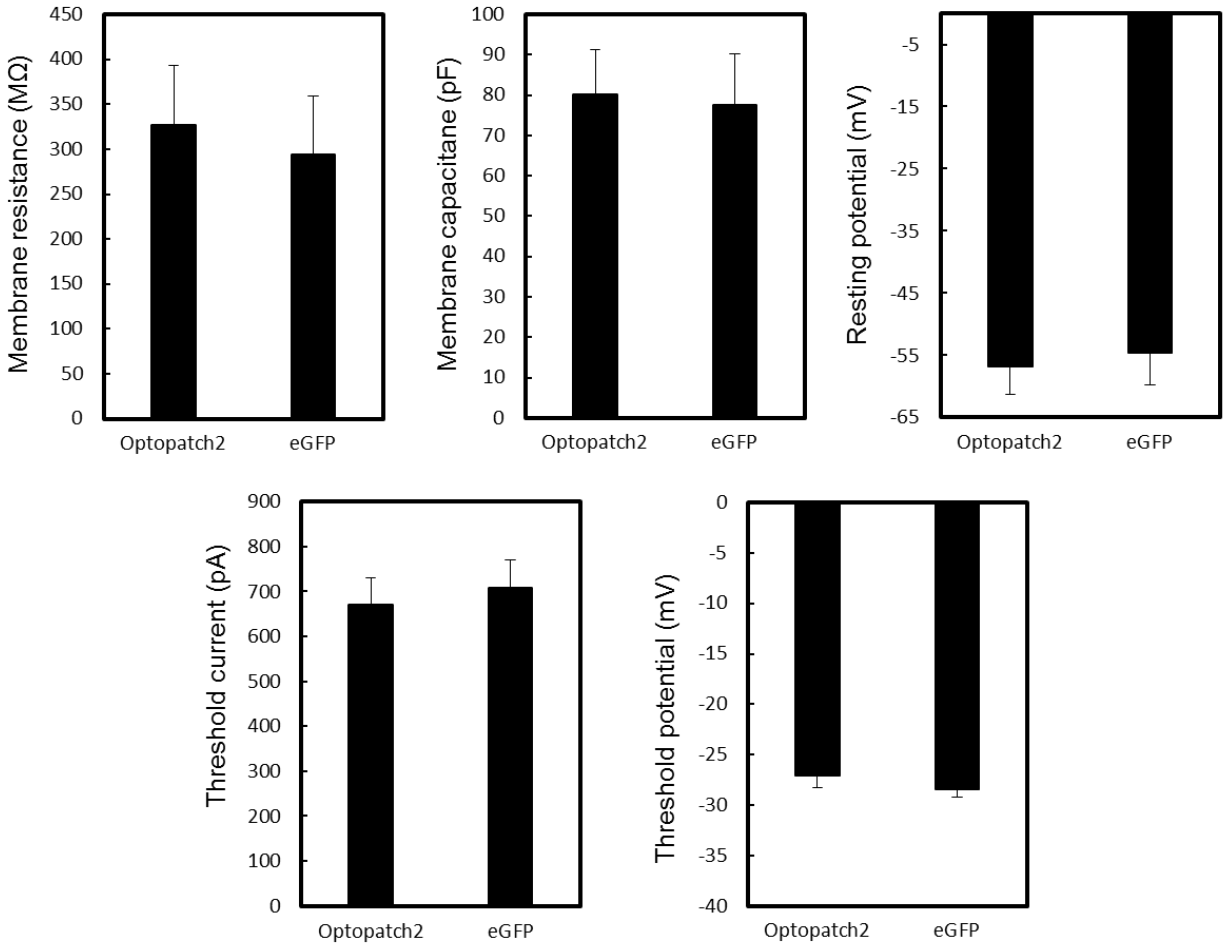

Effect of Optopatch expression on membrane electrical properties. Matched cultures were transfected via calcium phosphate on DIV 7 with either cytoplasmic eGFP or Optopatch2 in identical plasmids with a *CaMKII*α promoter. Expressing cells (n = 8 Optopatch2, n = 7 eGFP, DIV 15) were measured via whole-cell patch clamp. There was no significant difference in membrane resistance (P = 0.72), membrane capacitance (P = 0.87), or resting potential (P = 0.31) between Optopatch2 and eGFP expressing cells. Threshold current and potential for action potential initiation were determined by applying increasing steps in current (400-850 pA, 5 ms duration, repeated at 5 Hz). There was no significant difference in threshold current (P = 0.67) or potential (P = 0.38) between Optopatch2 and eGFP expressing cells. Error bars represent s.e.m. Statistical significance determined by two-tailed student's t-test or Mann–Whitney U test.

Supplementary Figure 12

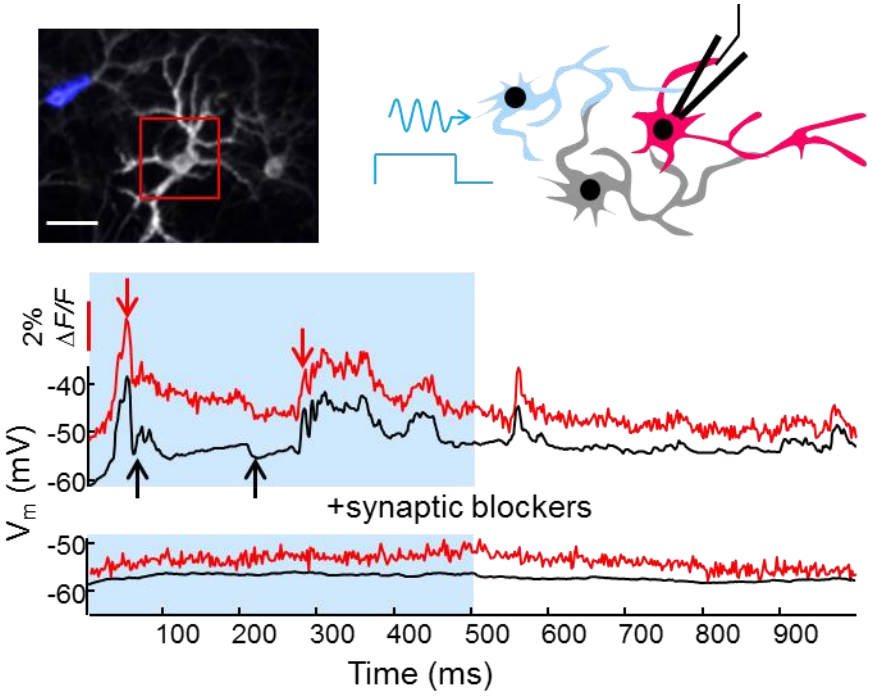

Optopatch measurements of post-synaptic responses. Top: Three cells expressing Optopatch2 were imaged via eGFP fluorescence (after conclusion of the experiment). The blue shading shows the region optically stimulated in the leftmost cell (488 nm, 35 mW/cm^2, 500 ms pulses) to stimulate network activity. The red square shows the camera field of view used for imaging QuasAr2 fluorescence. The membrane voltage of the cell within this region was simultaneously monitored via QuasAr2 fluorescence and via whole-cell patch clamp. Middle: Simultaneous patch clamp (black line) and fluorescence (red line) recording of subthreshold activity in the postsynaptic cell (640 nm exc., 1200 W/cm^2). The presence of optically induced EPSPs (red arrows) and IPSPs (black arrows) in the same cell indicates recruitment of other cells in the network. Bottom: Synaptic blockers (10 μM NBQX, 20 μM gabazine, 25 μM AP-V) eliminated the response in the postsynaptic cell.

Supplementary Figure 13

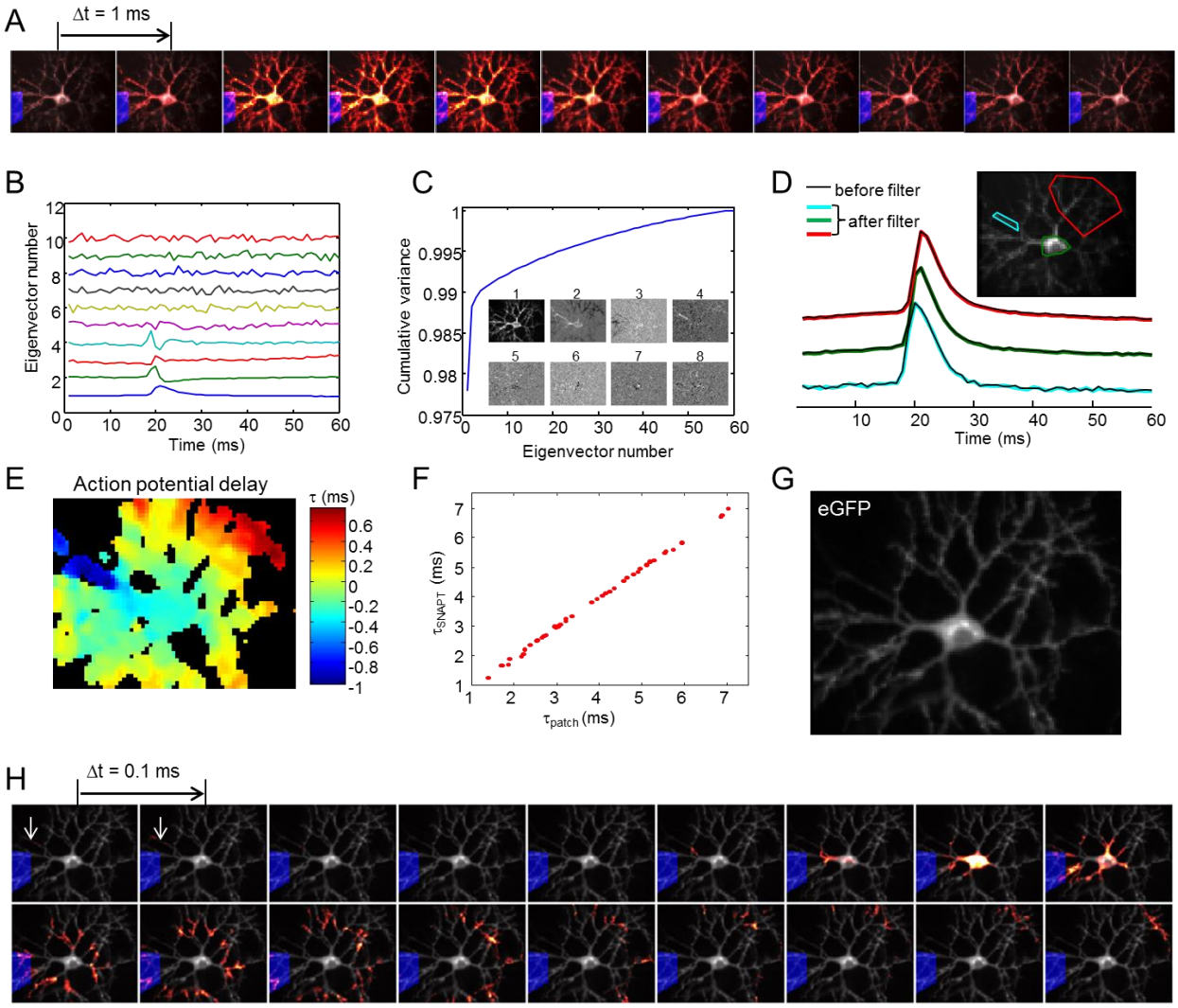

Sub-frame interpolation highlights subcellular timing differences in AP initiation. A) Patterned optical excitation (blue region) was used to induce between 100 and 400 APs. Fluorescence movies of individual APs were acquired at 1,000 frames/s, temporally registered and averaged. The sub-threshold depolarization is greatest at the location of the optical stimulus, and propagates passively through the cell until it crosses the AP initiation threshold. B) The movie of a mean AP was passed through a mild spatial filter, and then Principal Components Analysis (PCA) was applied to AP waveforms at individual pixels. The first 5 PCA eigenvectors accounted for > 99% of the pixel-to-pixel variation in AP waveforms; the remaining eigenvectors were noise. C) Cumulative variance of the fluorescence signal accounted for by the first *n* eigenvectors. In this example the cumulative variances explained by the first five eigenvectors were: 97.8%, 98.8%, 98.9%, 99.0%, and 99.1%. Inset shows projection of the spike movie onto each of the first eight eigenvectors. D) Comparison of AP waveforms before

and after the spatial and PCA smoothing operations. Black lines represent original movie, colored lines represent filtered data recorded in the axon (cyan), soma (green), and dendrites (red). E) Map of AP timing, calculated for the cell shown in (A) and (D). Here the timing was defined as the time to reach 50% of maximum intensity on the rising edge of the AP. Note the early timing in the axon initial segment on the left. F) Absolute accuracy of timing extracted by the sub-frame interpolation algorithm for voltage at the soma, compared to a simultaneously acquired patch clamp recording. The r.m.s. error between optically inferred and electrically recorded timing was 54 μs in this example. Note the absence of systematic offsets at the frame boundaries. G) High-resolution image of eGFP fluorescence, indicating CheRiff distribution. H) Frames from a sub-frame interpolated movie formed by mapping the timing information in (E) onto the high spatial resolution image in (G). White arrows mark zone of AP initiation in the presumed axon initial segment. Data is from the same cell as in **Fig. 3e**, with images rotated 90 °.

Supplementary Figure 14

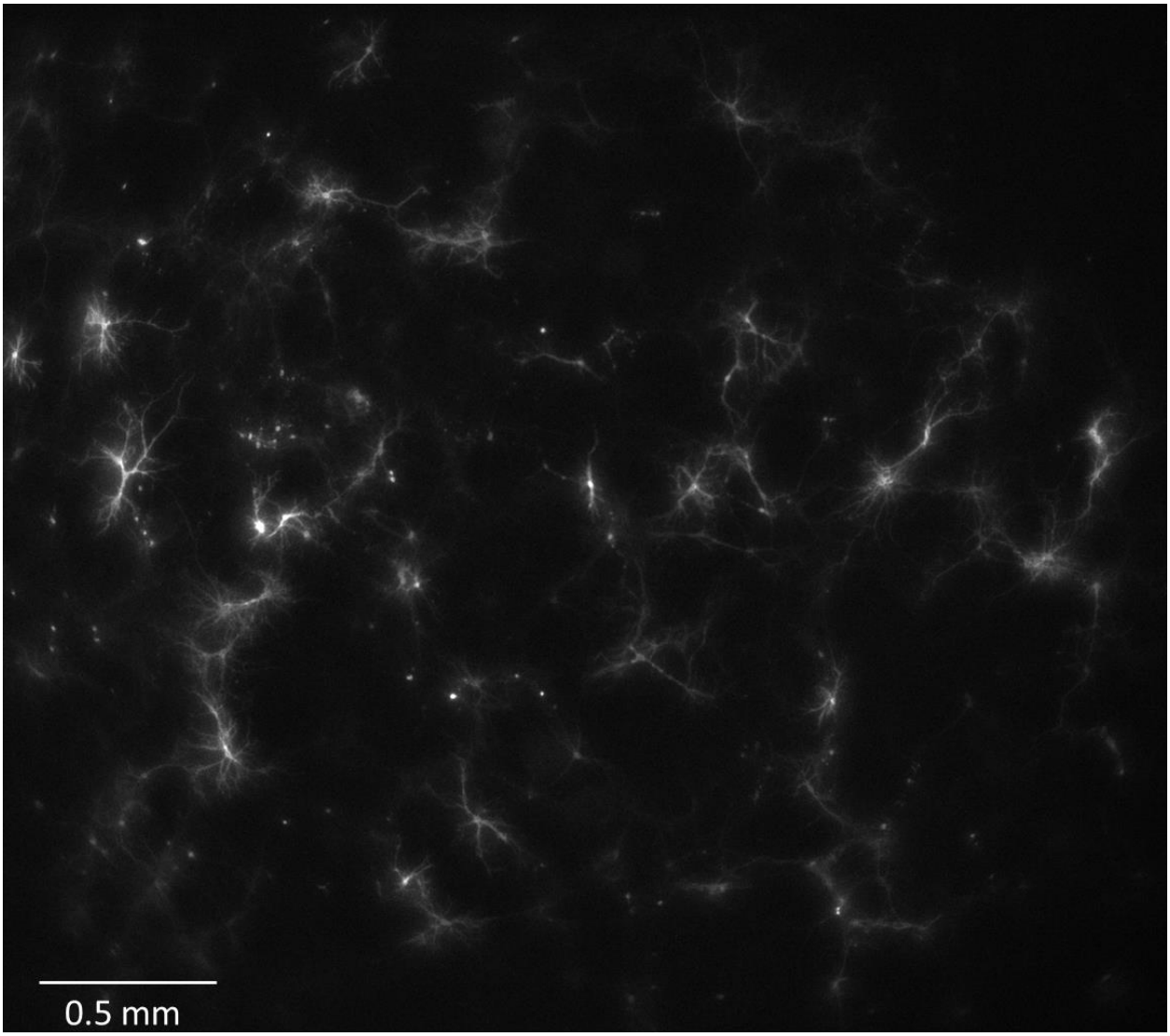

Low magnification optical system enables simultaneous imaging of many neurons. Neurons expressing Optopatch2, imaged via eGFP fluorescence. More than 50 cells are visible in this field of view. Limitations on data-rate from the camera required that the field of view be compressed in the vertical direction to 0.6 mm for optical recordings at 1 kHz, or to 1.2 mm for optical recordings at 500 Hz.

Supplementary Figure 15

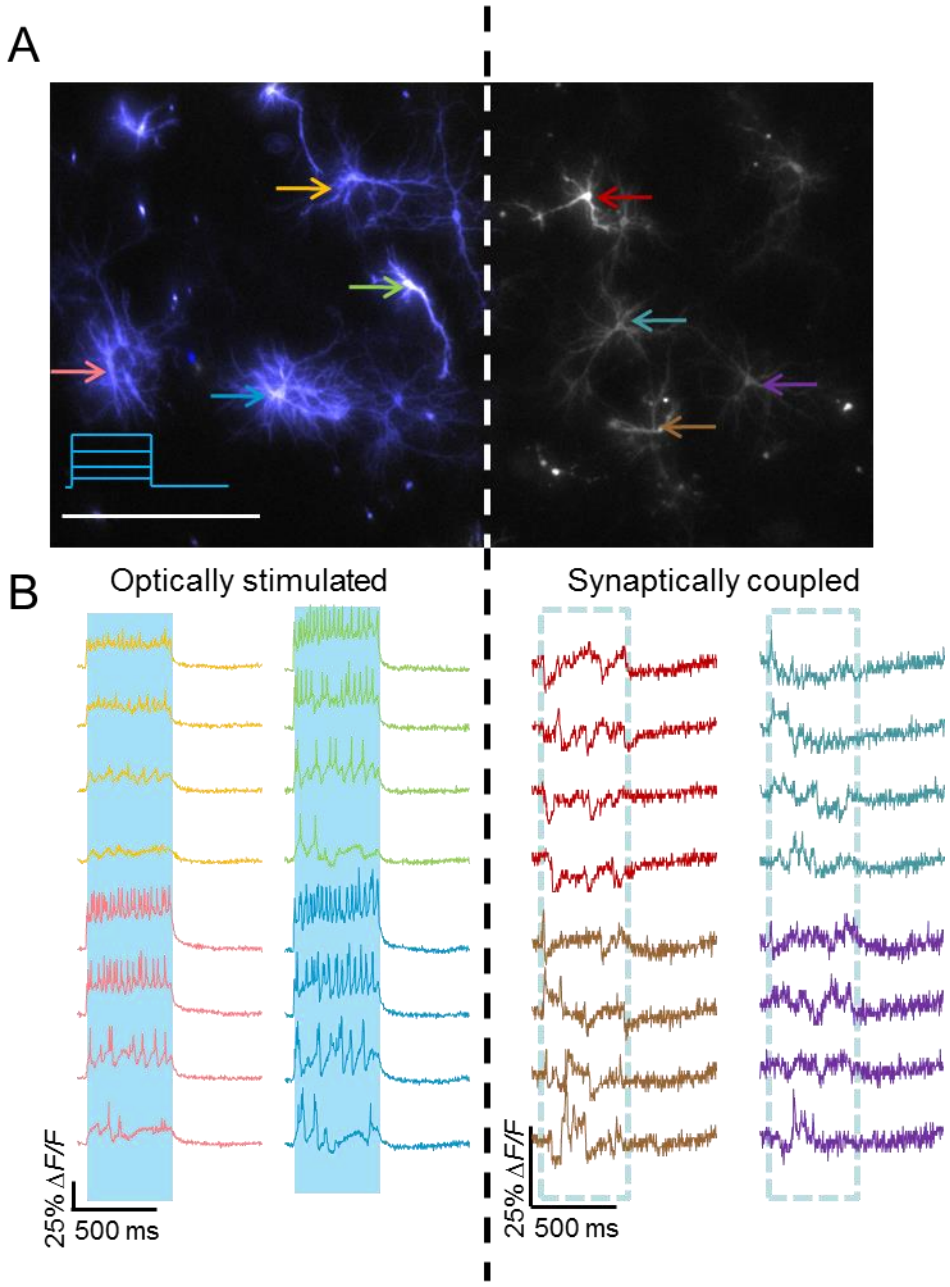

Optopatch measurements of network activity. A) Image of eGFP fluorescence in a culture of neurons expressing Optopatch2. The left half of the field (colored blue) was stimulated with blue light of increasing intensity (0.5 s, 1 to 10 mW/cm^2) and the whole field was illuminated with red light (100 W/cm^2). B) Left: fluorescence traces showing APs in the neurons indicated in (A) with correspondingly colored arrows. Right: synaptically induced activity in the indicated neurons which did not receive direct optical stimulation. Scale bar 500 μm.

Supplementary Figure 16

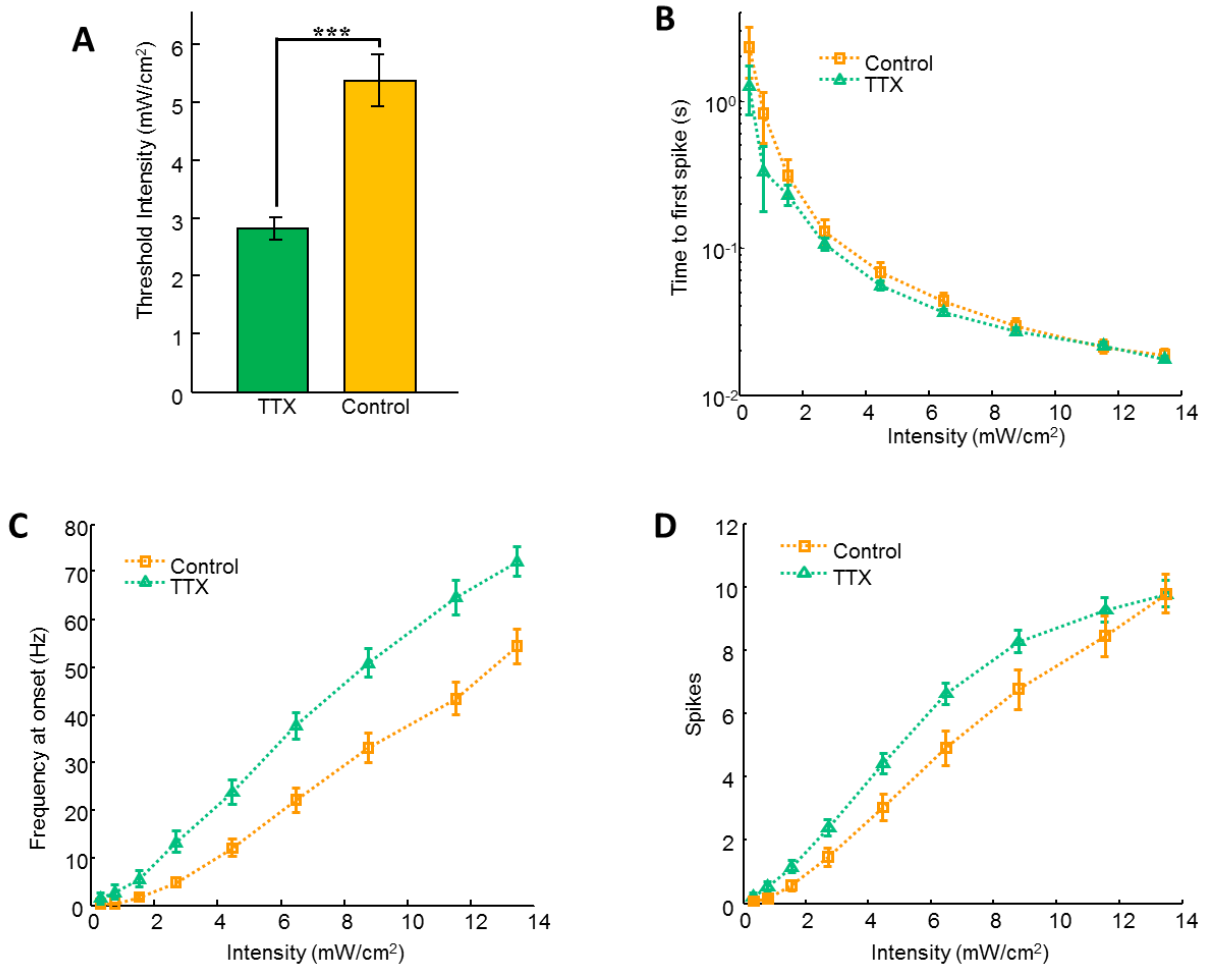

Homeostasis of intrinsic excitability in primary neurons induced by chronic exposure to TTX. Neurons expressing Optopatch2 were incubated in 1 μM TTX for 48 hours starting at 16 days post plating, and then tested in TTX-free imaging medium. Paired control dishes from the same culture were incubated with vehicle alone. Data from n = 75 control cells and n = 94 TTX-treated cells. QuasAr2 fluorescence was monitored (640 nm, 100 W/cm^2) while cells were illuminated with pulses of blue light (500 ms) of increasing intensity (0 to 14 mW/cm^2, repeated twice). A) Threshold blue light stimulation intensity to induce at least one AP in 500 ms. TTX treated cells had a significantly lower threshold than controls ($P = 5\times10^{-6}$). B) Time from onset of illumination to first spike. TTX-treated and control cells did not differ substantially by this measure. C) Spike frequency at onset (inverse time between first and second spike). TTX-treated cells fired faster than control cells ($P < 0.001$ for each stimulation intensity ≥ 2.7 mW/cm^2). D) Number of spikes during 500 ms stimulus window. TTX-treated cells had more spikes than control cells ($P < 0.01$ for stimulus intensities between 0.8 and 8.8 mW/cm^2). Error bars represent s.e.m. *** $P < 0.001$. Statistical significance determined by two-tailed student's t-test or Mann–Whitney U test.

Supplementary Figure 17

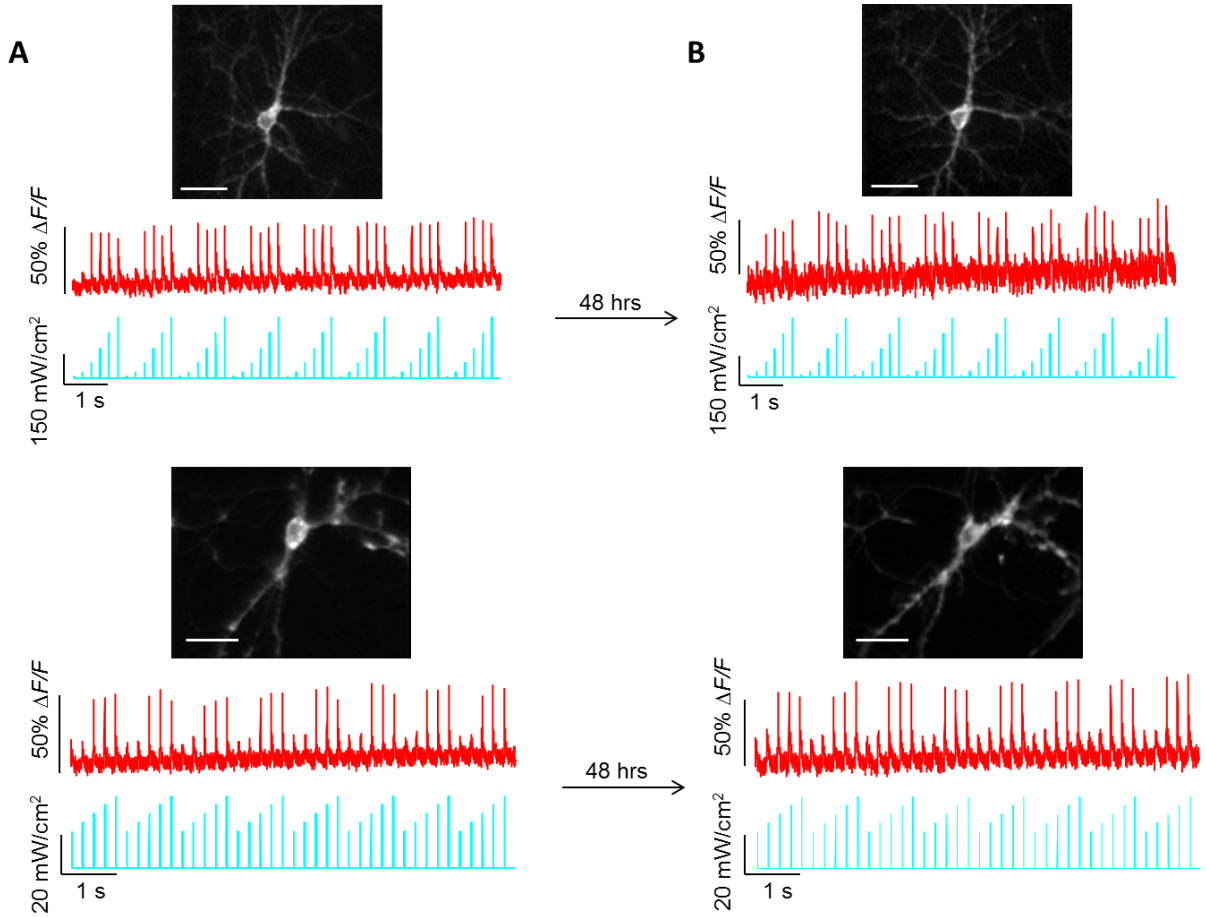

Repeated Optopatch recordings from neurons expressing Optopatch2. Images show mOrange2 fluorescence. Scale bar 40 μm. A) Primary rat hippocampal neurons were stimulated with pulses of blue light of increasing intensity, targeted to the soma (blue). Cells produced optically detected APs under the stronger stimuli. The stimulus and imaging protocol lasted 1 min. After the recording, the imaging medium was replaced with culture medium and the cells were returned to the incubator. B) 48 hrs later, the same cells were located in the microscope and the stimulus protocol was repeated. The cells responded similarly in the first and second trial. Paired recordings separated by 48 hrs were successful in n = 8 of 10 cells.

Supplementary Figure 18

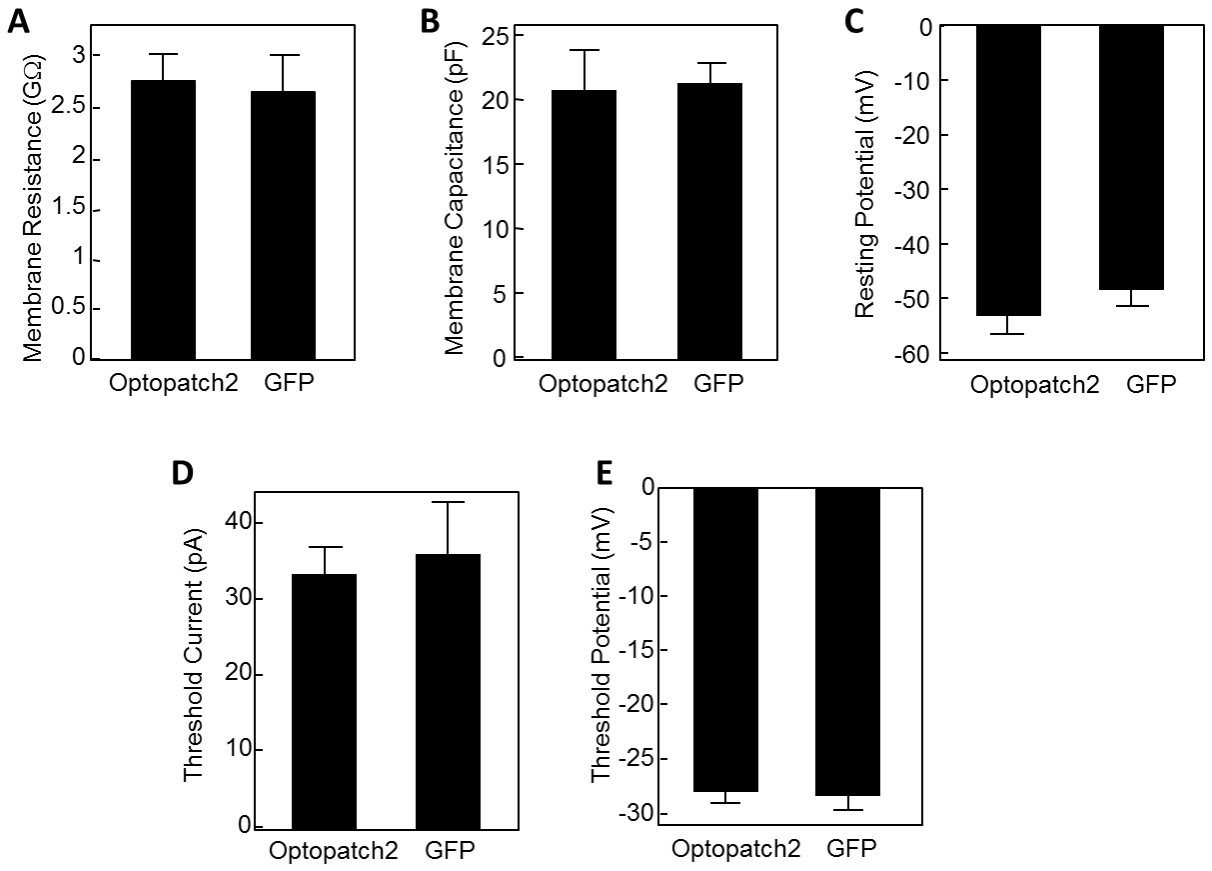

Effect of Optopatch expression on membrane electrical properties of hiPSC-derived neurons. Matched cultures were transfected via calcium phosphate on DIV 10 with either cytoplasmic eGFP or Optopatch2 in identical plasmids with a *CaMKII*α promoter. Expressing cells (n = 11 Optopatch2, n = 11 eGFP, DIV 20) were measured via whole-cell patch clamp. There was no significant difference in A) membrane resistance (P = 0.82), B) membrane capacitance (P = 0.88), or C) resting potential (P = 0.34) between Optopatch2 and eGFP expressing cells. Threshold current and potential for action potential initiation were determined by applying increasing steps in current (20-120 pA, 100 ms duration, repeated at 1 Hz). There was no significant difference in D) threshold current (P = 0.78) or E) potential (P = 0.43) between Optopatch2 and eGFP expressing cells. Error bars represent s.e.m. Statistical significance determined by two-tailed student's t-test or Mann–Whitney U test.

Supplementary Figure 19

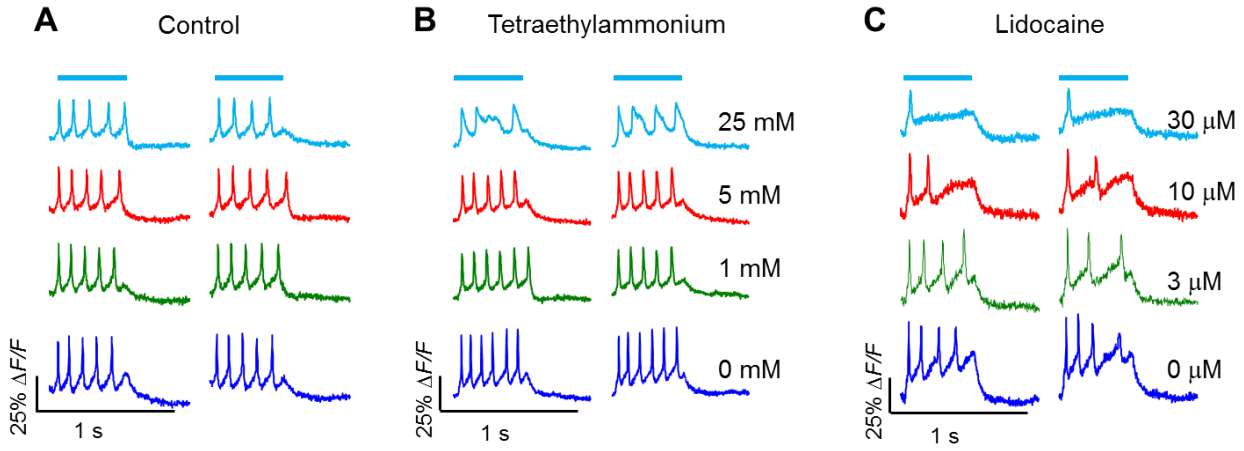

Influence of channel blockers on excitability of hiPSC-derived neurons. A) Human iPSC-derived neurons were excited with 500 ms pulses of blue light to initiate a train of APs. Repeated stimulation with blue light led to repeatable trains of APs. B) Representative AP trains with increasing concentrations of tetraethylammonium (TEA), a voltage-gated potassium channel blocker. TEA blocked repolarization after AP initiation. C) Representative AP trains with increasing concentrations of lidocaine, an activity-dependent sodium channel blocker. Lidocaine prevented repetitive firing.

Supplementary Figure 20

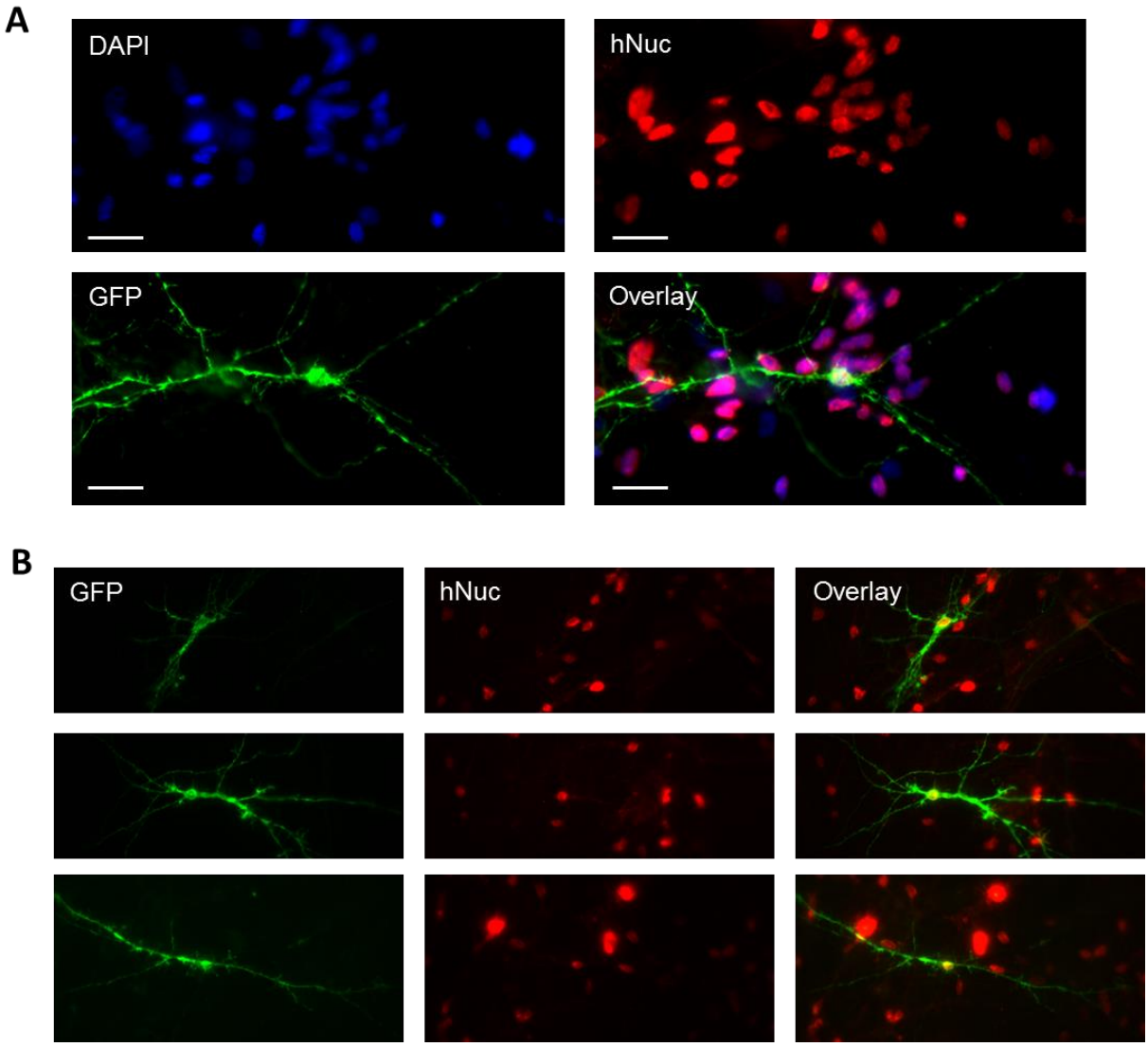

Immunostaining to validate human origin of hiPSC-derived neurons. A) Measurement of specificity of anti-human nuclear antigen 1 (*hNuc*) antibody for human cells. In a culture of hiPSC-derived neurons on rat glia, all nuclei were stained with DAPI (blue). A subset of these stained with *hNuc*, indicating two antigenically different populations. A subset of the *hNuc*-positive cells stained for GFP. These were hiPSC-derived neurons that had taken up and expressed the Optopatch construct. Scale bars 20 μm. B) Human iPSC-derived neurons used in experiments on homeostatic plasticity were fixed immediately after data acquisition and immunostained against eGFP to label transfected neurons and *hNuc* to label human nuclei. All eGFP expressing cells (277 of 277) showed colocalization of the *hNuc* with GFP.

Supplementary Figure 21

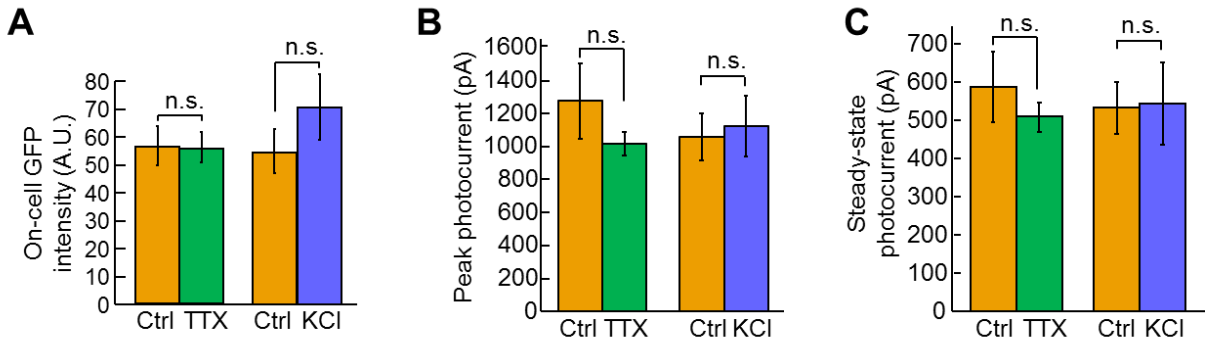

Tests of TTX or KCl chronic treatment on CheRiff expression and function in hiPSC-derived neurons. A) Fluorescence of eGFP can be used as a proxy for the expression level of CheRiff. Images of eGFP fluorescence were acquired for all cells used in HPIE measurements. The mean eGFP fluorescence intensity was quantified for each cell. There was no significant difference in intensity levels between TTX treated cells (n = 31 cells) and their untreated controls (n = 32 cells, P = 0.59). There was also no significant difference in intensity levels between KCl treated cells (n = 28 cells) and their untreated controls (n = 25 cells, P = 0.29). B) & C) Characterization of photocurrents in treated and untreated cells. Cells were transfected and treated identically to the optical HPIE experiments. Membrane voltage was held at V = -65 mV via manual patch clamp. Photocurrents were elicited by a blue light pulse (1 s, 488 nm, 500 mW/cm^2). There was no significant difference in peak or steady state photocurrents between TTX treated cells and untreated controls (n = 8 TTX treated cells, n = 10 untreated control cells, P = 0.31 for peak photocurrents, P = 0.44 for steady state photocurrents). There was also no significant difference in peak or steady state photocurrents between KCl treated cells and untreated controls (n = 7 KCl treated cells, n = 7 untreated control cells, P = 0.69 for peak photocurrents, P = 0.78 for steady state photocurrents**).** Error bars represent s.e.m. Statistical significance determined by two-tailed student's t-test or Mann–Whitney U test.

Supplementary Figure 22

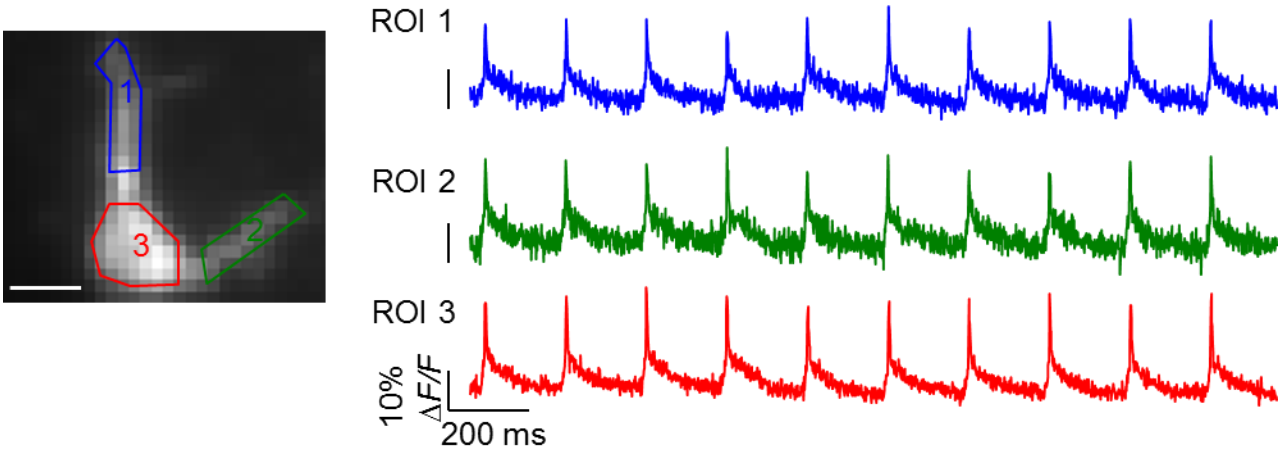

Subcellular optopatch measurements in organotypic brain slice. Optical recordings (640 nm, 1,200 W/cm^2 nominal incident intensity; 1 kHz frame rate on an EMCCD) of optically evoked action potentials (10 ms, 7.5 mW/cm^2, repeated at 5 Hz) in a neuron expressing Optopatch2 in a brain slice. Subcellular fluorescence was extracted by selecting regions of interest (ROIs) around two proximal dendrites and the cell body. Single-trial APs were seen clearly with high SNR in the dendrites, as well as the cell body. Scale bar 15 μm.

Supplementary Figure 23

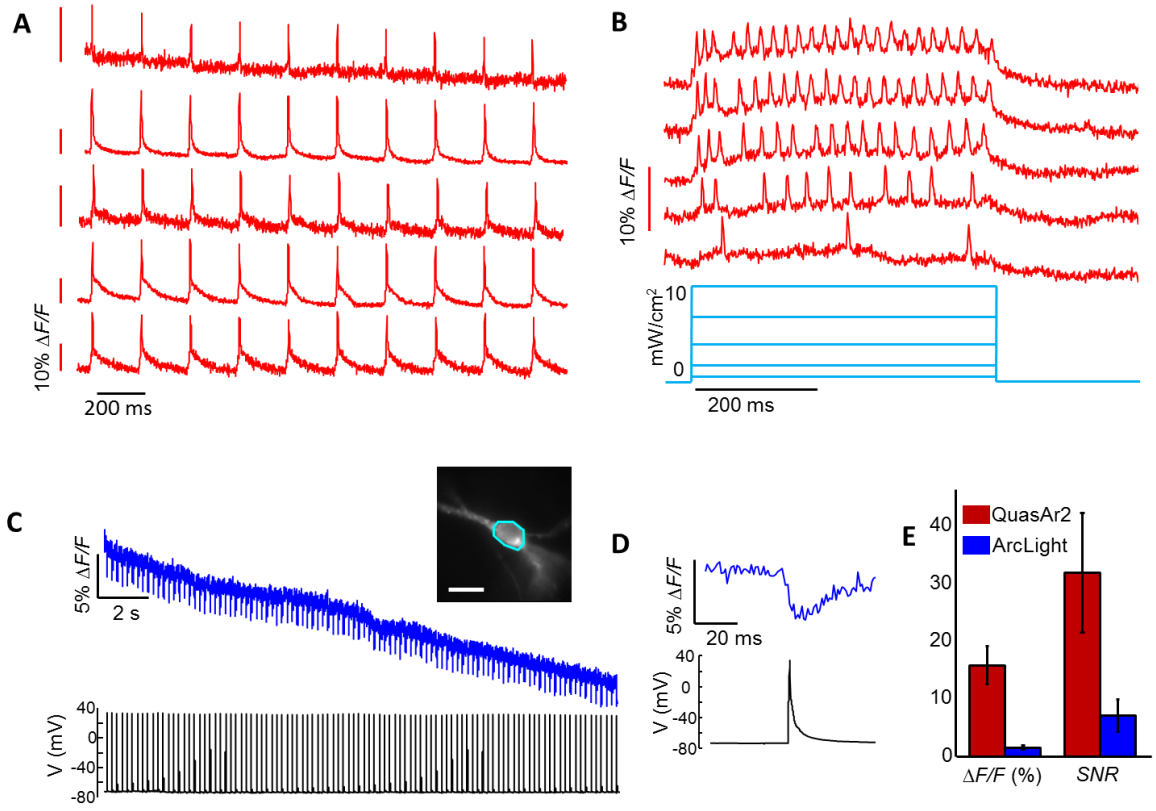

Optopatch and ArcLight measurements in organotypic brain slice. A) Optical recordings of optically evoked action potentials in five cells from separately prepared brain slices expressing QuasAr2. Differences in signal-to-noise ratio reflect differences in cell depth and in expression level. Action potentials were induced with blue light (10 ms, 7.5-15 mW/cm^2, repeated at 5 Hz) and whole-soma fluorescence was recorded at a frame rate of 1 kHz on an EMCCD camera (640 nm illumination 1,200 W/cm^2 nominal incident intensity, not corrected for light scatter). B) Sustained spiking in response to steps in blue light intensity (488 nm, 500 ms, increasing intensity from 1 to 10 mW/cm^2). QuasAr2 fluorescence was excited with illumination at 640 nm, 400 W/cm^2 incident on the sample, not corrected for scattering. C) Trace of fluorescence transients in a neuron expressing ArcLight A242 (488 nm, 50 W/cm^2) in response to a train of APs. Inset: Image of the neuron. Scale bar 20 μm. Cyan box shows ROI used to extract fluorescence from a high-speed (1 kHz frame rate) movie. D) Single-trial fluorescence response of ArcLight (blue) to a single AP (black). E) Comparison of QuasAr2 and ArcLight in brain slice. For detection of a single AP, QuasAr2 Δ*F/F* was 15.9 ± 3.0% (*n* = 7 cells), 10-fold larger than ArcLight Δ*F/F* (1.5 ± 0.4%, *n* = 6 cells). QuasAr2 SNR was 31.9 ± 9.5, over 4-fold larger than ArcLight SNR of 7.1 ± 2.8. Illumination conditions for E) were: ArcLight, 488 nm, 50 W/cm^2; QuasAr2, 640 nm, 1200 W/cm^2. Fluorescence was extracted by manual ROI selection of the soma for both ArcLight and QuasAr2. All fluorescent traces and Δ*F/F* calculations are presented without background subtraction or correction for photobleaching.

Supplementary Table 1

Protein Name	Quantum yield	Quantum yield relative to Arch D95N
Arch	N/A*	N/A*
Arch D95N	4×10^{-4}	1.0
QuasAr1	8×10^{-3}	19
QuasAr2	4×10^{-3}	10
Arch D95H/D106H	2×10^{-3}	4.2
Arch D95H/D106H/P60S	5×10^{-3}	12
Arch D95H/D106H/F161V	5×10^{-3}	13

* Due to the low light intensities used to determine QYs, fluorescence from Arch was not detected above baseline.

Quantum yields of Arch variants measured in solubilized protein. Fluorescence emission spectra were recorded with excitation at 600 nm. Details of sample preparation and measurement are given in **Methods**.

Supplementary Table 2

Mutant	Brightness (λ_{exc} = 640 nm)		τ_{up} (ms, -70 mV to +30 mV)			τ_{down} (ms, +30 mV to -70 mV)			Sensitivity (ΔF/F per 100 mV)
	0.7 W/cm^2	800 W/cm^2	τ_1	τ_2	% τ_1	τ_1	τ_2	% τ_1	
23 °C									
Arch(WT)	1	4.0	0.6	NA	NA	0.25	1.9	67%	40%
QuasAr1	15.2	10.3	0.05	3.2	94%	0.07	1.9	88%	33%
QuasAr2	3.4	3.4	1.2	11.8	68%	1.0	15.9	80%	90%
Arclight A242			17.4	123	39%	68	121	24%	-32%
34 °C									
QuasAr2			0.3	3.2	62%	0.3	4.0	73%	
Arclight A242			12	72	78%	21.5	NA	100%	

Spectroscopic and kinetic properties of Arch mutants and ArcLight. Brightness, response speed, and sensitivity were measured in HEK293 cells. Brightness and voltage sensitivity were comparable at 34 °C and 23 °C.

Supplementary Table 3

Mutant	Trafficking	Blue photocurrent (pA; peak, 500 mW/cm^2)	Red photocurrent (pA; 640 nm, 300 W/cm^2)	τ_{off} (ms)
sdChR-eGFP	×			
sdChR-TS-eGFP	✓	2470±170	38±4	26±2.9
CheRiff (sdChR-E154A-TS-eGFP)	✓	2030 ± 100	10.5±2.8	16±0.8

Spectroscopic and kinetic properties of *Scherffelia dubia* mutants. Photocurrents were measured in cultured rat hippocampal neurons under voltage-clamp at V_m = -65 mV. All quantities are represented as mean ± s.e.m. for n = 5 to 7 cells.

Supplementary Table 4

ChR variant	I_{max} (nA; 488 nm, 0.5 W/cm^2)		t_{on} (ms)	τ_{des} (ms)	τ_{off} (ms)	EPD50 (mW/cm^2)	Red photocurrent (pA; 640 nm, 300 W/cm^2)	Red light depolarization (mV), 300 W/cm^2
	Peak	Steady state						
CheRiff	2.0±0.1	1.33±0.08	4.5±0.3	400±40	16±0.8	22±4	10.5 ± 2.8	2.3 ± 0.3
ChIEF	0.9±0.1	0.81±0.10	18±1.8	51±10	15±2		15.0 ± 2.5	2.1 ± 0.15
ChR2 H134R	1.1±0.1	0.65±0.09	9.1±0.7	40±5	25±4	43±4	2.2 ± 0.9	1.0

Comparison of CheRiff, ChIEF, and ChR2 H134R. All parameters were measured in cultured rat hippocampal neurons. Photocurrents were measured under voltage-clamp at V_m = -65 mV. All quantities are represented as mean ± s.e.m. for n = 5 to 7 cells. EPD50 = intensity for 50% maximal photocurrent.

Supplementary Table 5

	Peak CheRiff photocurrent (pA)	Fluorescence	
		QuasAr1	QuasAr2
Blue (500 mW/cm^2)	2030±100	0.02	0.017
Red (300 W/cm^2)	10.5±2.8	3.0	1

Optical crosstalk between CheRiff and QuasAr channels in Optopatch constructs. Photocurrents were measured in cultured rat hippocampal neurons under voltage-clamp at V_m = -65 mV. Photocurrents are represented as mean ± s.e.m. for n = 5 to 7 cells. Fluorescence values were measured in HEK293 cells. Fluorescence of QuasAr constructs is normalized to the value for QuasAr2 illuminated at 640 nm, 300 W/cm^2.

Supplementary Table 6

Name	Sequence
Fw_XbaI_Arch	CGACTCTAGAATGGACCCCATCGCTCTGCAGGCTGGTTACGACCTGCTGGGTGACGGC
RV_Arch	TGCTACTACCGGTCGGGGCTCGGGGGCCTC
FW_Arch_FP	GAGGCCCCCGAGCCCCGACCGGTAGTAGCAATGGTGAGCAAGGGCGAGGAG
RV_HindIII_FP	GATGAAGCTTTTACTT GTACAGCTCGTCCATGCCG
FW_Arch_95X	CTATTATGCCAGGTACGCCHVSTGGCTGTTTACCACCCCAC
FW_Arch_106X	CCCCACTTCTGCTGCTGNRCCTGGCCCTTCTCGCTAA
FW_Arch_95N	ATTATGCCAGGTACGCCAATTGGCTGTTTACCACC
FW_Arch_95C	CTA TTA TGC CAG GTA CGC CTGTTG GCT GTT TAC CAC CCC AC
FW_Arch_95Q	CTA TTA TGC CAG GTA CGC CCAGTG GCT GTT TAC CAC CCC AC
FW_Arch_106C	CCCCACTTCTGCTGCTGTGCCTGGCCCTTCTCGCTAA
Fw_Arch_106E	CCCCACTTCTGCTGCTGGAGCTGGCCCTTCTCGCTAA
Fw_BamHI_Kozak_Arch	CGACGGATCCACCATGGACCCCATCGCTCTGCAGGC
RV_FP_ERex_stp_XbaI	GATGTCTAGATTATTCATTCTCATAACAAAACTTGTACAGCTCGTCCATGCCG
FW_BamHI_Kozak_Arch_ValSer	TGGGATCCACCATGGTAAGTATCGCTCTGCAGGCTGGTTAC
RV_FP_TS	ATCCAGGGGGATGTACTCGCCTTCGCTTGTGATTCTACTCTTGTACAGCTCGTCCATGCCG
RV_TS_ER export_ stop_EcoRI	GATGGAATTCTTATACTTCATTCTCATAACAAAATCCACCTACATTTATGTCTATTTGATCCAGGGGGATGTACTCGCC

Oligonucleotides used in directed evolution of QuasArs

References

1. Enami, N. *et al*. Crystal structures of archaerhodopsin-1 and-2: Common structural motif in archaeal light-driven proton pumps. *J. Mol. Biol.* **358**, 675-685 (2006).

2. Kralj, J. M., Douglass, A. D., Hochbaum, D. R., Maclaurin, D. & Cohen, A. E. Optical recording of action potentials in mammalian neurons using a microbial rhodopsin. *Nat. Methods* **9**, 90-95 (2011).

3. Mattis, J. *et al*. Principles for applying optogenetic tools derived from direct comparative analysis of microbial opsins. *Nat. Meth.* **9**, 159-172 (2011).

4. Lin, J. Y., Lin, M. Z., Steinbach, P. & Tsien, R. Y. Characterization of engineered channelrhodopsin variants with improved properties and kinetics. *Biophys. J.* **96**, 1803-1814 (2009).